Original Article

Journal of Intelligent Material Systems and Structures

Journal of Intelligent Material Systems and Structures
1–11
© The Author(s) 2015
Reprints and permissions:
sagepub.co.uk/journalsPermissions.nav
DOI: 10.1177/1045389X15590273
jim.sagepub.com
SAGE

A design of active elastic metamaterials for control of flexural waves using the transformation method

Yangyang Chen[1], Jin Hu[2] and Guoliang Huang[1]

Abstract

The ability to control flexural wave propagation is of fundamental interest in many areas of structural engineering and physics. Metamaterials have shown a great potential in subwavelength wave propagation control due to their inherent local resonance mechanism. In this study, we propose a transformation method to derive the material properties of a flexural waveguide and implement the functionality based on a design of active elastic metamaterials. The numerically demonstrated flexural waveguide can not only steer an elastic wave beam as predicted from the transformation method but also exhibit various unique properties including extraordinary wave beam deflection and tunabilities over a broad frequency range and various steering directions. The waveguide is equipped with an array of active elastic metamaterials composed of the electrorheological elastomer subjected to adjustable electric fields. Such metamaterial-based waveguides provide a new design methodology for guided wave signal modulation devices and could be useful for applications such as tunable beam steering, high signal-to-noise sensors, and structural health monitoring.

Keywords

active elastic metamaterials, transformation method, flexural wave control

Introduction

The lowest antisymmetric Lamb waves, flexural waves, in a plate have been extensively employed in structural health monitoring thanks to their capability of long-range and through-thickness interrogation of structures (Guo and Cawley, 1993; Lemistre and Balageas, 2001; Zhu et al., 2013). To achieve high-resolution damage detection, controlling of flexural wave propagation paths is extremely essential in both emitting and receiving processes. For example, when a monitored object is not on the ray direction of the flexural wave propagation, a waveguide structure could steer the wave to a desired direction. On the other hand, flexural wave focusing can increase the signal-to-noise ratio of sensor signals and therefore improve the damage detection resolution (Wu et al., 2011; Yan et al., 2013). Designing a waveguide device to achieve full control of flexural waves would be of great benefit to the development of structural health monitoring and new sensors.

A transformation method has been initially proposed for controlling electromagnetic (EM) waves and determining the relation between the functionality of a device and the material pattern in the space (Pendry et al., 2006). Because of the similarity between the EM wave and the acoustic wave, the transformation method has also been proposed for acoustic wave controlling (Chen and Chan, 2007, 2010). The key principle of transformation methods is based on the form-invariance of governing equations under an arbitrary transformation mapping. However, for elastic waves, Milton et al. (2006) showed that Navier's equations cannot maintain the form-invariance under a general spatial mapping, which means that methodologies applied in EM or acoustic transformations cannot be directly applied to control elastic waves. Specifically, by conducting the transformation of a governing equation in a polar coordinate system, Farhat et al. (2009) suggested a cylindrical cloaking for plate bending

[1]Department of Mechanical & Aerospace Engineering, University of Missouri–Columbia, Columbia, MO, USA
[2]School of Information and Electronics, Beijing Institute of Technology, Beijing, China

Corresponding author:
Guoliang Huang, Department of Mechanical & Aerospace Engineering, University of Missouri–Columbia, Columbia, MO 65211, USA.
Email: huangg@missouri.edu

Downloaded from jim.sagepub.com by guest on July 28, 2015

waves. However, a systematical transformation method for controlling flexural waves has not been explicitly proposed based on an arbitrary transformation mapping. Recently, based on the assumption of local affine transformations, Hu et al. (2011) and Chang et al. (2011) proposed an approximate method to establish the transformation relations for elastic waves. The method was numerically illustrated as a powerful tool to control elastic waves at high frequencies or in small material-gradient elastic media. The method will serve as the theoretical transformation foundation both as a tool to provide flexural wave control on the general transformation mapping and determine the properties of the transformed materials.

Although the transformed parameters derived by the transformation method are sometimes simple in form, the physical realization of the material parameters varying continuously with position over a broad range of values is still an immense difficulty (Greenleaf et al., 2009; Schmiele et al., 2010). Acoustic/elastic metamaterials (EMMs), consisting of resonant elements, significantly enlarge the space for effective property selection due to the dispersive nature of their unit cells (Christensen and De Abajo, 2012; Huang et al., 2009; Liu et al., 2011; Zhu et al., 2011, 2014). They are usually organized at a smaller scale than the wavelength and have bands with high momentum modes that are equivalent to high effective parameters or frequency bands with negative effective properties that manifest as band gaps, which make them feasible for the physical realization of elastic wave control. However, to achieve the wave steering over a broad frequency range, locally resonant metamaterials have to be redesigned or reformed on either microstructural geometries or constituent materials because the effective properties are closely related to the microstructure of the resonator. This challenging task makes metamaterials extremely difficult for real-time practical applications. Recently, active acoustic metamaterials, whose effective properties can be tuned under external stimuli, have been developed to realize a wide range of effective densities, which is not possible with passive components alone (Baz, 2009). Among different approaches, smart materials with controllable moduli under externally electric or magnetic loads are typically integrated into the microstructures to promptly tune effective density and modulus of the acoustic metamaterials (Chen et al., 2014; Tang et al., 2004; Xu and Wu, 2014; Yeh, 2007; Zhou and Chen, 2013).

In this article, we theoretically demonstrate a design and numerical simulations of a flexural waveguide based on the active EMM. First, the transformation method for the flexural wave in the plate is developed and the transformed material properties are analytically derived. The physical realization of the transformed medium is proposed by an array of active EMMs in the form of discretization and truncation. The tunable effective properties are accomplished by integrating an electrorheological (ER) elastomer subjected to adjustable electric fields in the microstructure of the local resonator. Finally, the numerical simulation is conducted to demonstrate tunability and flexibility of the proposed waveguide over a broad frequency range and various steering directions without altering the microstructures. The study could have a very profound application in extraordinary wave beam steering and structural health monitoring.

A transformation method of controlling flexural waves in plates

In general, the governing equation of flexural waves in an inhomogeneous isotropic plate can be expressed in the Cartesian coordinate system as (Leissa, 1969)

$$\nabla^2(D\nabla^2 w) - (1-\nu)\left(\frac{\partial^2 D}{\partial y^2}\frac{\partial^2 w}{\partial x^2} - 2\frac{\partial^2 D}{\partial x \partial y}\frac{\partial^2 w}{\partial x \partial y} + \frac{\partial^2 D}{\partial x^2}\frac{\partial^2 w}{\partial y^2}\right) + \rho h\frac{\partial^2 w}{\partial t^2} = 0 \quad (1)$$

where $\nabla^2 = (\partial^2/\partial x^2) + (\partial^2/\partial y^2)$; $w(x, y)$, $\rho(x, y)$, $h(x, y)$, and $\nu(x,y)$ are the out-of-plane displacement field of the neutral plane, mass density, thickness, and Poisson's ratio of the plate, respectively, and the bending stiffness is defined as $D(x,y) = (E(x,y)h^3(x,y))/(12(1-\nu^2(x,y)))$ with $E(x, y)$ being the Young's modulus. The transformation method can be applied to a general plate; however, in this study, Kirchhoff plate theory is adopted for the interested frequency range because the wavelength is much larger than the thickness of the plate, where the thickness shear deformation effect can be ignored. For $D(x, y)$ being a constant D_0, the governing equation can be reduced as

$$D_0\nabla^2(\nabla^2 w) + \rho h\frac{\partial^2 w}{\partial t^2} = 0 \quad (2)$$

where the phase velocity is defined as $c_p = (D_0\omega^2/\rho h)^{1/4}$.

In the study, the transformation method based on the assumption of a general mapping as a series of local affine deformations will be adopted and extended for controlling bending wave propagation in a plate. The basic idea of the method will be briefly reiterated for a general transformation mapping $\mathbf{x}' = \mathbf{x}'(\mathbf{x})$ from a virtual two-dimensional (2D) space Ω to a physical 2D space Ω', as shown in Figure 1. In the virtual space Ω, a local Cartesian frame $\mathbf{e}_i$ is established at a point $\mathbf{x} = (x, y)^{\mathrm{T}}$ and another local Cartesian frame $\mathbf{e}'_i$ is formed at a point $\mathbf{x}' = (x', y')^{\mathrm{T}}$ in the physical space Ω'. Under the affine deformation, the deformation gradient tensor of the mapping $\mathbf{A} = \nabla_{\mathbf{x}}\mathbf{x}'$ can be decomposed into a rigid rotation tensor $\mathbf{R}$ and a pure stretch tensor

Downloaded from jim.sagepub.com by guest on July 28, 2015

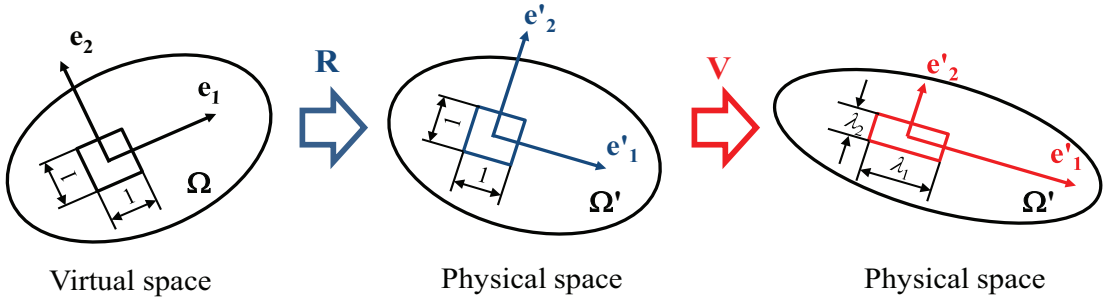

Figure 1. Transformation mapping interpreted by local affine deformations.

$\mathbf{V}$ ($\mathbf{A} = \mathbf{VR}$), where $\mathbf{V} = \lambda_1 \mathbf{e}'_1 \otimes \mathbf{e}'_1 + \lambda_2 \mathbf{e}'_2 \otimes \mathbf{e}'_2$ with λ_1 and λ_2 being the principal stretches. Similarly, any physical and material quantities in the system should follow the decomposition of the transformation as

$$\mathbf{V_q R}: \quad q \to \mathbf{q}', \quad q = w, E, \rho, h, \nu \tag{3}$$

where $\mathbf{V_q}$ is a scaling tensor of quantity q. Equation (3) implies that their transformed quantities can be derived under the same rotation but different stretches in its local space element. The constraints on the form-invariance of the transformed governing equation as well as the energy conservation conditions will provide a way to determine the stretch tensor $\mathbf{V_q}$.

For the purpose of physical realization, a conformal transformation mapping is considered, which indicates that the principle stretches satisfy $\lambda_1 = \lambda_2 = \lambda$ and the resultant materials are isotropic. Under the conformal mapping, the transformed governing equation can be written locally with respect to the local Cartesian system $\mathbf{e}'_i$ as

$$\nabla'^2(D'\nabla'^2 w') - (1-\nu')\left(\frac{\partial^2 D'}{\partial y'^2}\frac{\partial^2 w'}{\partial x'^2} - 2\frac{\partial^2 D'}{\partial x'\partial y'}\frac{\partial^2 w'}{\partial x'\partial y'} + \frac{\partial^2 D'}{\partial x'^2}\frac{\partial^2 w'}{\partial y'^2}\right) + \rho' h'\frac{\partial^2 w'}{\partial t^2} = 0 \tag{4}$$

where $\nabla'^2 = (\partial^2/\partial x'^2) + (\partial^2/\partial y'^2)$ and $D'(x', y') = (E'(x', y')h'^3(x', y'))/(12(1-\nu'^2))$ and w', ρ', h', E', and ν' are the corresponding out-of-plane displacement field, mass density, thickness, Young's modulus, and Poisson's ratio of the plate in the transformed physical space Ω', respectively. For the flexural wave, the transformations of the displacement, thickness, and material parameters in the local Cartesian frame $\mathbf{e}'_i$ according to equation (3) can be assumed as

$$w' = aw \tag{5a}$$

$$\rho' = b\rho \tag{5b}$$

$$h' = ch \tag{5c}$$

$$E' = dE \tag{5d}$$

$$\nu' = e\nu \tag{5e}$$

where the scaling factors a, b, c, d, and e are the unknown parameters to be determined.

Based on differential relations between two spaces $\partial/\partial x' = (1/\lambda)\partial/\partial x$ and $\partial/\partial y' = (1/\lambda)\partial/\partial y$, equation (4) can be rewritten in the initial space Ω as

$$\frac{ac^3 d}{\lambda^4}\left(\frac{\partial^2}{\partial x^2} + \frac{\partial^2}{\partial y^2}\right)\left[D(1-mu^2)/(1-e^2 mu^2)\left(\frac{\partial^2 w}{\partial x^2} + \frac{\partial^2 w}{\partial y^2}\right)\right] - (1-e\nu)\frac{ac^3 d}{\lambda^4}\left(\frac{\partial^2 D}{\partial y^2}\frac{\partial^2 w}{\partial x^2} - 2\frac{\partial^2 D}{\partial x\partial y}\frac{\partial^2 w}{\partial x\partial y} + \frac{\partial^2 D}{\partial x^2}\frac{\partial^2 w}{\partial y^2}\right) (1-mu^2)/(1-e^2 mu^2) + abc\rho h\frac{\partial^2 w}{\partial t^2} = 0 \tag{6}$$

Comparing equation (6) to equation (1) by the form-invariance, the relations of the scaling factors are determined as

$$\frac{dc^2}{b} = \lambda^4 \tag{7a}$$

$$e = 1 \tag{7b}$$

Thus, the scaled Poisson's ratio remains the original value during the mapping to ensure the form-invariance of the governing equation of an inhomogeneous plate. For the 2D transformation, it is natural to assume the thickness of the plate to be unchanged as $c = 1$. Therefore, we have $d/b = \lambda^4$, which can also be expressed as

$$\frac{E'}{\rho'} = \lambda^4 \frac{E}{\rho} \tag{8}$$

On the other hand, potential and kinetic energy conservations need to be satisfied during the mapping. In the virtual space, potential and kinetic energies in a Kirchhoff plate can be expressed as

$$PE = \frac{1}{2}D\left\{(\nabla^2 w)^2 - 2(1-\nu)\left[\frac{\partial^2 w}{\partial x^2}\frac{\partial^2 w}{\partial y^2} - \left(\frac{\partial^2 w}{\partial x\partial y}\right)^2\right]\right\}\mathrm{d}x\mathrm{d}y \tag{9a}$$

$$KE = \frac{1}{2}\rho h\left(\frac{\partial w}{\partial t}\right)^2 \mathrm{d}x\mathrm{d}y \tag{9b}$$

Downloaded from jim.sagepub.com by guest on July 28, 2015

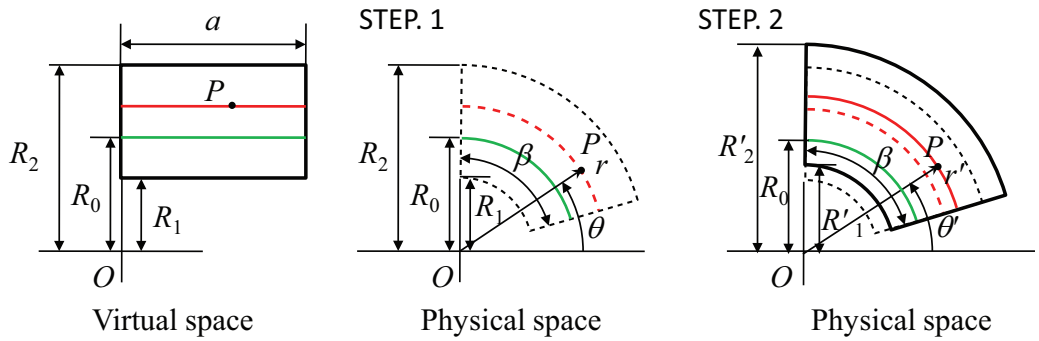

Figure 2. Two-step transformation of an isotropic waveguide.

In the physical space, potential and kinetic energies of the plate are

$$PE' = \frac{1}{2}D' \left\{(\nabla'^2 w')^2 - 2(1-\nu')\left[\frac{\partial^2 w'}{\partial x'^2}\frac{\partial^2 w'}{\partial y'^2} - \left(\frac{\partial^2 w'}{\partial x' \partial y'}\right)^2\right]\right\} \mathrm{d}x'\mathrm{d}y' \tag{10a}$$

$$KE' = \frac{1}{2}\rho' h' \left(\frac{\partial w'}{\partial t}\right)^2 \mathrm{d}x'\mathrm{d}y' \tag{10b}$$

By combing scaling factors in equations (5a) to (5e) and the conformal transformation condition, equations (10a) and (10b) can be rewritten in the initial space as

$$PE' = \frac{1}{2}\frac{a^2 c^3 d}{\lambda^2} D(1-mu^2)/(1-e^2 mu^2) \left\{(\nabla^2 w)^2 - 2(1-e\nu)\left[\frac{\partial^2 w}{\partial x^2}\frac{\partial^2 w}{\partial y^2} - \left(\frac{\partial^2 w}{\partial x \partial y}\right)^2\right]\right\} \mathrm{d}x\mathrm{d}y \tag{11a}$$

$$KE' = \frac{1}{2}a^2 bc\lambda^2 \rho h \left(\frac{\partial w}{\partial t}\right)^2 \mathrm{d}x\mathrm{d}y \tag{11b}$$

Based on the energy conservation, the relation of the scaling factors and principle stretch can also be derived, which is in the same form of equation (7). The result further validates the accuracy of the transformation method. In addition, the scaling factor of the transformed displacement, a, can also be determined as

$$a = c\sqrt[4]{bd} \tag{12}$$

It should be mentioned that transformation relations of flexural waves in the plate are different for elastic waves in the isotropic bulk media, where the transformation relation is $E'/\rho' = \lambda^2 E/\rho$ (Chang et al., 2011).

Mapping design of a beam steering of flexural waves

The proposed transformation method is then used for the design of a flexural waveguide to steer flexural waves propagating along desired directions. In order to demonstrate this, we consider a rectangular plate in the virtual space with width $b = (R_2 - R_1)$ and length a, respectively, as shown in Figure 2. To achieve the conformal mapping, a two-step transformation mapping will be conducted. In the first step, the plate is transformed into the arc shape with a polar angle β. It is easily shown that there is only rescaling in the θ direction during the transformation, and this stretch can be obtained by comparing the arc length of the waveguide βr with its original length a.

Therefore, two principle stretches at each point are

$$\lambda_r^{\mathrm{I}} = 1 \tag{13a}$$

$$\lambda_\theta^{\mathrm{I}} = \frac{\beta r}{a} = \frac{r}{R_0} \tag{13b}$$

where the superscript I represents the first-step transformation and $r = R_0$ is the arc where the length is unchanged during the transformation as $a = \beta R_0$. According to equation (13), this transformation will result in an anisotropic medium. To achieve a conformal mapping, a second-step transformation will be implemented to further adjust stretches in the r direction as

$$\lambda_{r'}^{\mathrm{II}} = \frac{\mathrm{d}r'}{\mathrm{d}r} \tag{14a}$$

$$\lambda_{\theta'}^{\mathrm{II}} = \frac{r'}{r} \tag{14b}$$

where II indicates the second-step transformation. Therefore, the total isotropic stretches in θ' and r' directions can be written as

$$\lambda = \lambda_r^{\mathrm{I}} \lambda_{r'}^{\mathrm{II}} = \lambda_\theta^{\mathrm{I}} \lambda_{\theta'}^{\mathrm{II}} \tag{15}$$

By substituting equations (14a) and (14b) into equation (15), we have

$$\lambda = \frac{\mathrm{d}r'}{\mathrm{d}r} = \frac{r'}{R_0} \tag{16}$$

and the required material parameters of the flexural waveguide can be determined as

Downloaded from jim.sagepub.com by guest on July 28, 2015

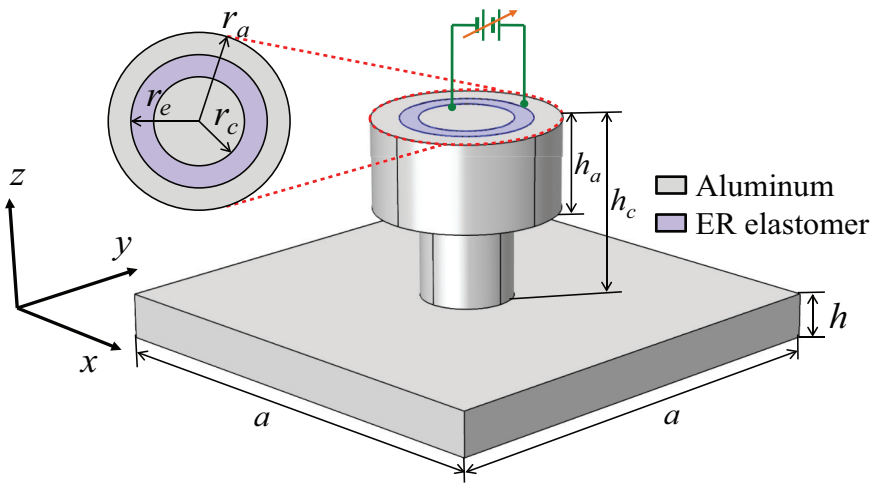

Figure 3. Unit cell of the active EMM surface-bonded on the plate.

$$\frac{E'}{\rho'} = \left(\frac{r'}{R_0}\right)^4 \frac{E}{\rho} \tag{17}$$

From equation (17), it can be concluded that the flexural waveguide can be achieved by finding materials with extremely gradient modulus or mass density, which is difficult to achieve using conventional materials. With the boundary condition that the arc length is unchanged, that is, $r' = R_0$, the transformation function $f(r)$ can be determined as

$$r' = f(r) = R_0 e^{\frac{r-R_0}{R_0}} \tag{18}$$

An active EMM for the flexural waveguide

In this section, an active EMM is proposed for physical realization of a material with tunable effective mass density, and thus for actively steering of flexural waves over a broad frequency range. The unit cell of the active EMM is schematically shown in Figure 3, where an active resonator is equipped with an ER elastomer annulus sandwiched between an aluminum annular ring and an aluminum cylinder. The resonator is surface-bonded on the top of the host plate. In the figure, a and h are the side length and the thickness of the unit lattice of the aluminum host plate, respectively. The radii and the height of the aluminum cylinder are denoted as r_c and h_c, respectively. The height and outer radii of the ER elastomer and aluminum annulus are represented by h_a, r_e, and r_a, respectively.

The working mechanism of the EMM can be briefly described as follows. When a bending wave propagates in the host plate with the surface-bonded EMM, the outer aluminum ring will be vibrated up and down with respect to the plate, and the ER elastomer will undergo shear mode deformation. With the presence of the anti-resonant motion of the outer aluminum ring with respect to the host plate, the flexural wave energy is trapped in the resonator and an omnidirectional wave band gap will be observed, which can be interpreted by the negative effective mass density of the system (Huang et al., 2009; Huang and Sun, 2009). In addition, the tunability and flexibility of the active EMM can be accomplished by tuning the shear modulus of the ER elastomer annulus under timely adjustable electric fields along the radial direction without altering the microstructures.

ER elastomers are soft elastomers by dispersing micrometer-size filler particles with high electrical permittivity and have adjustable rheological properties upon external electric loading, which induce stiffening or softening modulus of the elastomers. The relation between dynamic shear modulus of the ER elastomer, G, and applied electric field of magnitude, $\bar{E}$, can be approximately expressed as (Liu and Shaw, 2001; Zhou and Chen, 2013)

$$G = G_0\left[1 + \left(\frac{\bar{E}}{E_0}\right)^2\right] \tag{19}$$

where G_0 is the shear modulus without electric field, and E_0 is a reference electric field. Based on the model presented by Wei et al. (2011), the effects of visoelastic properties of the ER elastomer are very small in the interested frequency range, and therefore, the imaginary portion of the shear modulus of the ER elastomer is not considered in this study.

The numerically based effective medium method is used for determination of the out-of-plane effective mass density of the EMM (Zhu et al., 2011, 2014). By imposing the time-harmonic displacement constraints with $U_x = 0$, $U_y = 0$, and $U_z = Ae^{i\omega t}$ on the external surrounding boundaries, the effective mass density can be extracted as

Downloaded from jim.sagepub.com by guest on July 28, 2015

Table 1. Unit cell geometrical and material parameters of the active EMM.

Geometrical properties (mm)		Material properties	
a	5	Mass density (aluminum)	2700 kg/m^3
h	1.5	Lamé's first parameter (aluminum)	51 GPa
r_a	2	Shear modulus (aluminum)	26 GPa
r_e	0.7	Mass density (ER elastomer)	1000 kg/m^3
r_c	0.5	Lamé's first parameter (ER elastomer)	1532 kPa
h_a	2	G_0	64 kPa
h_c	1.8	E_0	1.3 kV/mm

ER: electrorheological.

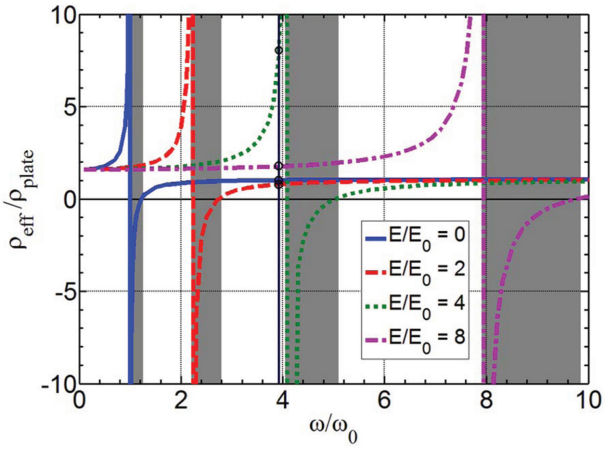

Figure 4. Effective mass density of the EMM under various magnitudes of electric fields.

$$\rho_{\text{eff}} = -\frac{F_z}{\omega^2 A V} \tag{20}$$

where F_z is the effective resultant force, and V is the volume of the unit cell.

Figure 4 shows the normalized effective mass densities of the proposed EMM under various magnitudes of applied electric fields by the finite element software, COMSOL Multiphysics. In the figure, ω_0 is the resonant frequency of the outer aluminum ring with $\bar{E} = 0$, and the microstructure dimensions and constitute material properties of the EMM are listed in Table 1.

As shown in the figure, the effective mass density reaches positive infinity at the resonant frequency and immediately turns to the negative infinity, then gradually approaches to a positive constant value at higher frequencies. Negative effective mass densities (shaded areas) can be found near the resonant frequency, that is, $\omega = \omega_0 - 1.3\omega_0$, when $\bar{E} = 0$. It can also be observed that the frequency range of the negative effective mass density can be shifted by changing the magnitudes of applied electric fields. For example, when $\bar{E} = 2E_0$, $4E_0$, and $8E_0$, the frequency range is shifted to $2.2\omega_0 - 2.8\omega_0$, $3.9\omega_0 - 5.1\omega_0$, and $8.1\omega_0 - 9.8\omega_0$, respectively. It is understandable because the shear modulus of the ER elastomer is increased with the increase in the magnitude of electric field according to equation (19), which will result in the shift of the resonant frequency. It is also noted that the frequency range of the negative effective mass density increases with the increase in the magnitude of the electric field. Finally, an extremely gradient distribution of effective mass density of the EMM can be accomplished by applying various magnitudes of electric fields at different frequencies. For example, as shown in the figure at $\omega = 3.9\omega_0$, the normalized effective mass density can be varied as 1.008, 0.7874, 7.555, and 1.758, respectively, when the electric field is tuned to be $\bar{E} = 0$, $2E_0$, $4E_0$, and $8E_0$, respectively, which provides a potential solution for wave steering devices. It should be mentioned that the tunability of the effective mass density through electric fields could be implemented very fast and in real time, which opens a new way for many practical applications of the active EMM.

As discussed in the previous section, for a conformal mapping, the transformed medium for the flexural waveguide should possess the in-plane isotropic properties. To investigate wave behavior of the proposed EMM, iso-frequency contours of the flexural wave under an electric field are shown in Figure 5. The contours are plotted in the first Brillouin zone and in the normalized wavenumber space. In the figure, microstructure dimensions and constitute material properties of the EMM are the same as those listed in Table 1, and magnitude of the applied electric field is $\bar{E} = 8E_0$. The unit of the frequency is kilohertz. For all the wave vectors $\mathbf{k} = (k_x, k_y)$ in the first Brillouin zone, we can numerically calculate a series of functions $\omega = g(k_x, k_y)$ by applying the Bloch–Floquet periodic boundary conditions to the unit cell, which are denoted as iso-frequency curves. The iso-frequency curves can provide rich information about the wave propagation characteristics of the considered domain for the EMM, which is different from the dispersion curves to illustrate the passing and stop bands along the appropriate wave vector path. The direction of wave propagation can be easily obtained by displaying these angles on polar plots. The group velocity of wave motion in a 2D EMM structure is given as

Downloaded from jim.sagepub.com by guest on July 28, 2015

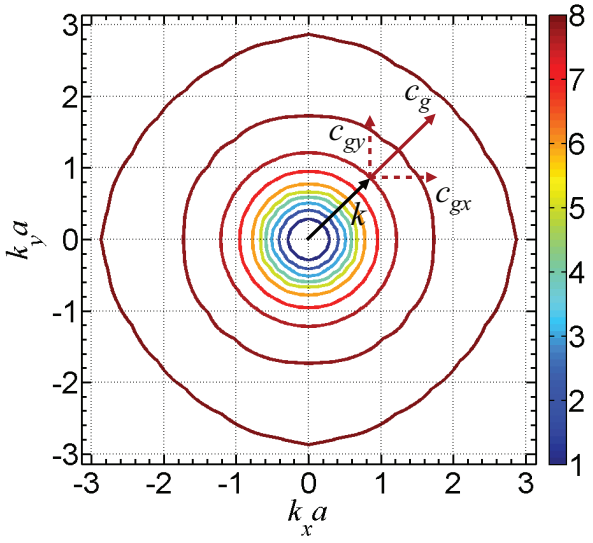

Figure 5. Iso-frequency contours of flexural waves of the active EMM.

$$c_{gx} = \frac{\partial \omega}{\partial k_x} \tag{21a}$$

$$c_{gy} = \frac{\partial \omega}{\partial k_y} \tag{21b}$$

For 2D EMMs, the characteristics of the wave propagation may be visualized in either of the following two ways: the energy flow is along the line of the steepest ascent on the iso-frequency surface or, equivalently, normal to the ω = constant lines on a contour plot of the iso-frequency surface. In this figure, nearly perfect circular contours are found at all interested frequencies, which illustrate the isotropic property of the proposed EMM because the group velocity vectors are collinear to the directions of wave propagation varying between 0° and 360°. Similar wave phenomena can also be observed for the EMM under different electric fields.

Numerical simulations and discussions

For the flexural waveguide application, since no homogeneous material exists that can reflect these properties in equation (17) based on the proposed mapping technique, we suggest a design to achieve such spatially varying properties using discrete distributions of active EMMs to perform the function. Control of the electric field adjusts the shear modulus of the ER elastomer which determines the dynamic density of the metamaterial. In this section, numerical simulations of the proposed flexural waveguide in a plate from the transformation method will be first conducted; in the meantime, the numerical simulation of the waveguide will be demonstrated using an array of surface-bonded active EMMs. Specifically, tunability and flexibility of

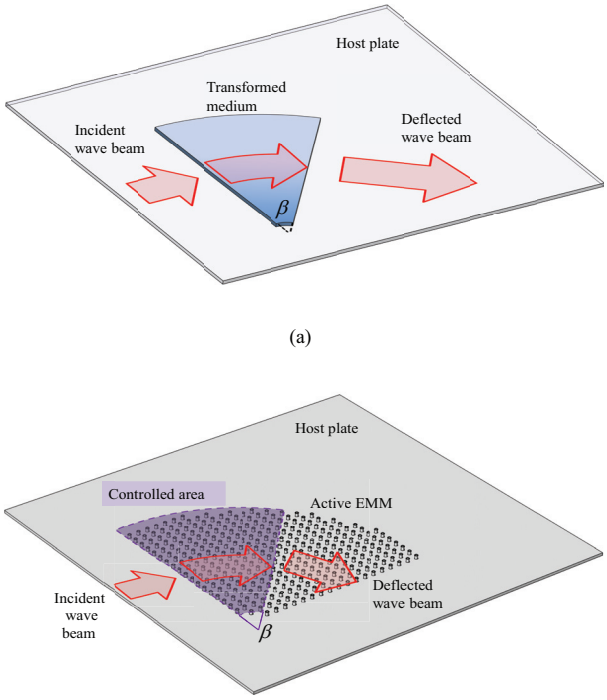

Figure 6. (a) Schematic of a flexural waveguide with a deflection angle β by the transformation method and (b) numerical simulation of a flexural waveguide equipped with an array of active EMMs.

the waveguide are discussed for the extraordinary wave steering over a broad frequency range.

Figure 6(a) shows the schematic model of the flexural waveguide with an arbitrary steering angle β by the transformation method. According to equation (17), there exist many options for material property selection of the transformed medium. For the ease of the physical realization, the relationship of the transformed medium and the host plate is selected as

$$E' = E \tag{22a}$$

$$\rho' = \left(\frac{R_0}{r'}\right)^4 \rho \tag{22b}$$

As illustrated in the figure, an incident flexural wave beam is launched toward the designed waveguide, and the wave is then steered along the waveguide with a beam deflection angle β. Figure 6(b) shows the numerical simulation of the waveguide using an array of the proposed active EMMs with a 90° circular sector. The mass density profile of the waveguide from the transformation method will be approximately truncated by the discretely distributed EMMs under various electric fields. The shear modulus of the ER elastomer and applied electric fields are numerically determined through the wave dispersion analysis. For example, the

Downloaded from jim.sagepub.com by guest on July 28, 2015

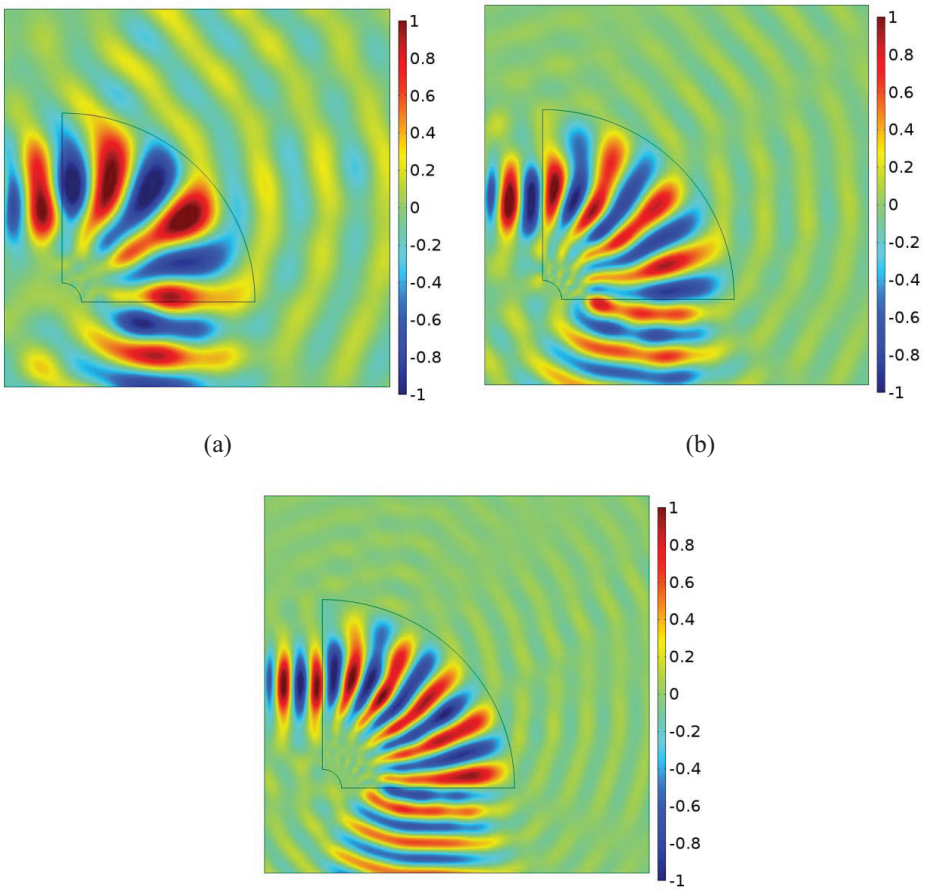

Figure 7. Normalized out-of-plane wave field of a 90° flexural waveguide with material parameters from transformation method at different incident frequencies: (a) 15 kHz, (b) 30 kHz, and (c) 50 kHz.

wavenumber can be determined from the spatially varying densities (equation (17)) at a point as

$$k_b(x,y) = \left(\frac{\rho(x,y)h\omega^2}{D}\right)^{\frac{1}{4}} \tag{23}$$

from which the shear modulus or the magnitude of the applied electric field of the ER elastomer can then be iterated by matching the calculated eigenfrequency to the incident frequency.

For the array of EMMs with a 90° sector, as shown in Figure 6(b), the beam deflection angle β ($0° < \beta < 90°$) can be actively adjusted by properly selecting the controlled area of the EMM. The out-of-plane component of the displacement field associated with the flexural wave propagating in the plate with the designed waveguide is calculated. Figure 7 shows the out-of-plane wave field of the flexural waveguide with the deflection angle being 90° based on the transformation method at the frequencies of 15, 30, and 50 kHz, respectively. In the model, perfectly matched layers (PMLs) on the host plate are adopted to simulate infinite boundaries for flexural wave propagation. The material parameters of the host plate are the same as those listed in Table 1. The waveguide is designed with the inner and outer radii of the circular sector (R_1' and R_2') being 10 and 100 mm, respectively. The material properties of the transformed medium are selected according to equation (22). A harmonic antisymmetric Gaussian displacement profile is launched along the left edge of the plate. It can be observed that the direction of flexural waves can almost be deflected to 90° for different frequencies. Small reflections are found on the interfaces between the waveguide and the background plate, due to the material mismatch between the host medium and transformed medium. In addition, scattered waves in the host plate leaking from the waveguide are also observed, which is caused by the width expansion of Gaussian beam. Specifically, when the incident frequency is increased from 15 to 50 kHz, the scattered wave becomes nearly invisible.

For the physical realization of the waveguide, an array of active EMMs is proposed. Figure 8 shows the numerical demonstration of the flexural waveguide

Downloaded from jim.sagepub.com by guest on July 28, 2015

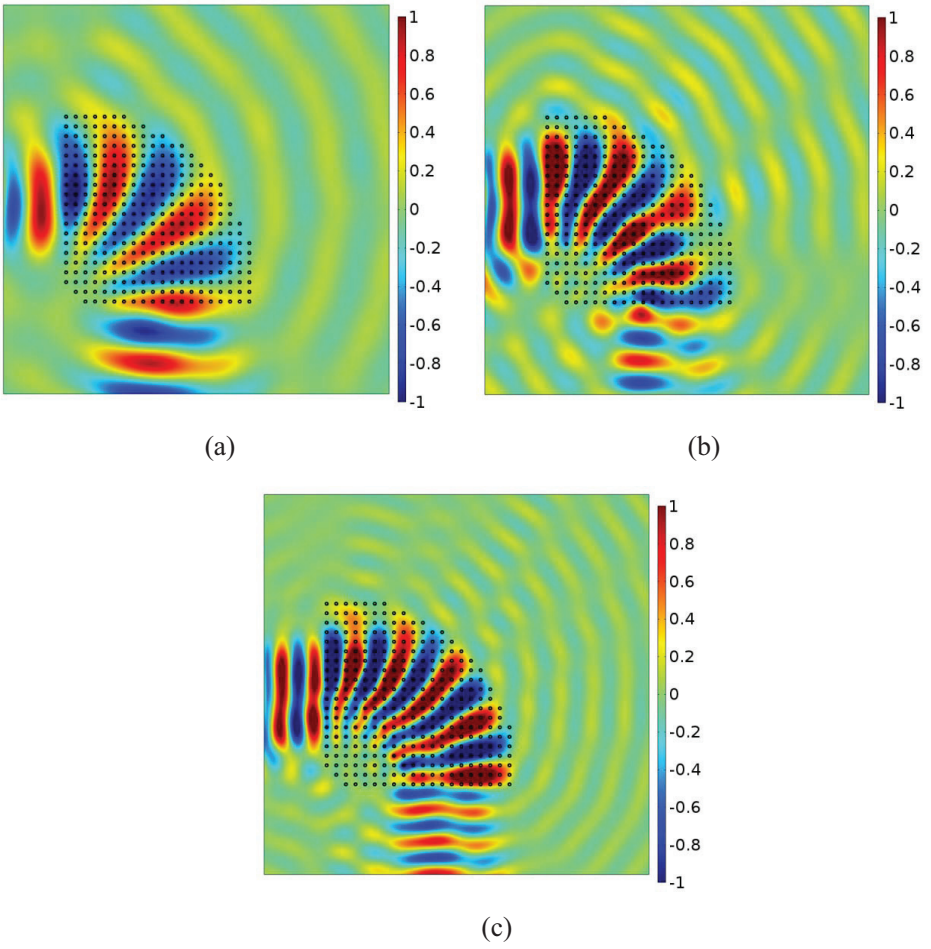

Figure 8. Normalized out-of-plane wave field of a 90° flexural waveguide equipped with an array of active EMMs at different incident frequencies: (a) 15 kHz, (b) 30 kHz, and (c) 50 kHz.

using the active EMM at different operating frequencies of 15, 30, and 50 kHz, respectively. For the active EMM, the outer radius of the aluminum ring r_a is selected as 0.9 mm, and other geometrical and material parameters are the same as those used in Figures 4 and 5. In the simulation, the required mass density profiles at different frequencies are approximated by the discretely distributed EMM through actively adjusting the applied electric field on the ER elastomer without altering the microstructure. It can be found that flexural waves are indeed steered into 90° as desired at all frequencies. Very good agreement with results predicted from the transformation method is observed, which shows the feasibility of the proposed active EMM. It is noted that interior scattering waves within the discretely distributed EMM nearly vanish because of the unique subwavelength feature of the proposed EMM compared with the wavelength of the operating frequency in the host plate.

Figure 9 shows the out-of-plane wave field of the flexural waveguide based on the proposed EMM at the operating frequency of 15 kHz with the deflection angle being 15°, 45°, and 60°, respectively. In the simulation, the material and geometrical parameters of the active EMM are the same as those used in Figure 8. As illustrated in the figure, the deflection angle can be flexibly tuned by applying electric fields on the selected areas (shaded areas) of the active EMM without altering the microstructures. The implied wave mechanism is that the effective mass density in the unselected area of the EMM is close to the mass density of the host plate at the operating frequency; therefore, the effects on the flexural wave propagation due to the bonded EMM can be ignored. We anticipate the active EMM to be capable of steering arbitrary elastic beams to provide remarkable flexibility and open new exciting possibilities in a variety of elastic-based applications ranging from damage imaging to sensor device design.

Summary

In this article, we have designed the flexural waveguide that can fully control the flexural wave propagation in the plate. The transformation method for the flexural wave in the plate is first developed and the transformed material properties are analytically derived. The

Downloaded from jim.sagepub.com by guest on July 28, 2015

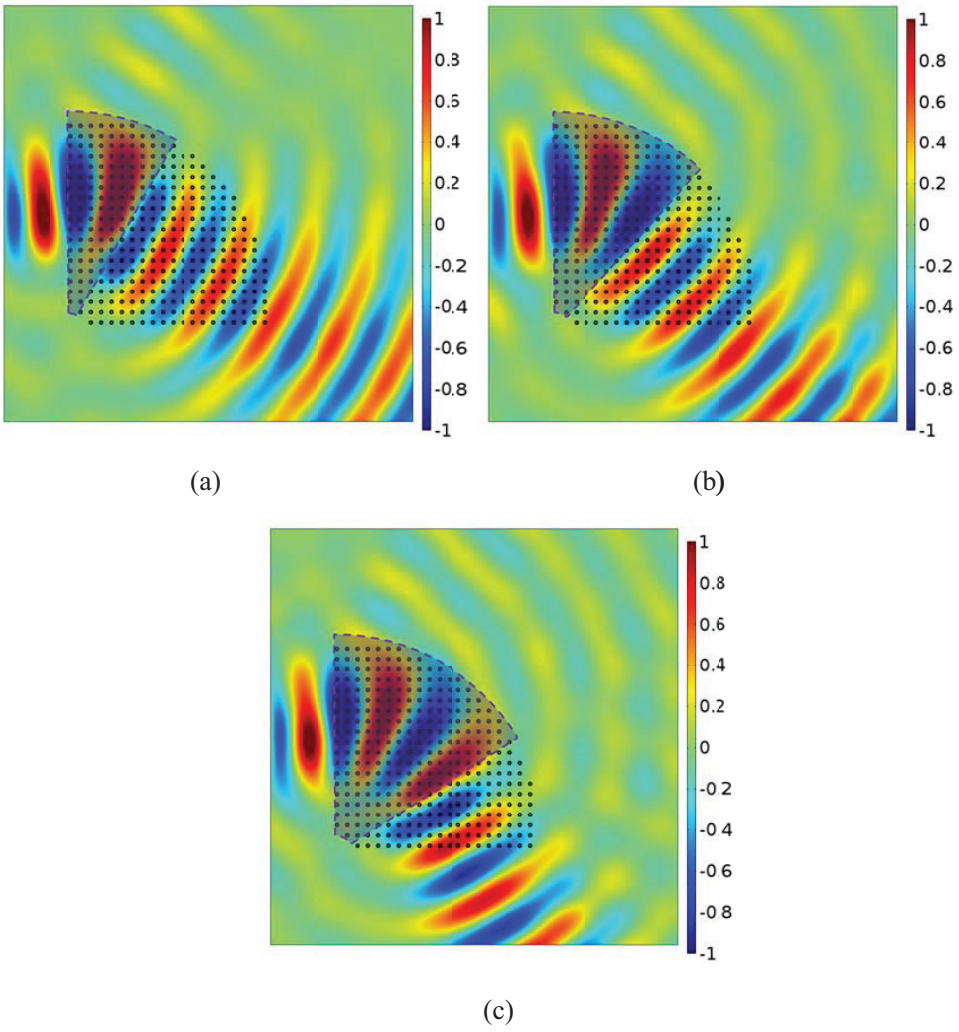

Figure 9. Normalized out-of-plane wave field of the flexural waveguide with controlled active EMMs at the operating frequency of 15 kHz with various deflection angles: (a) 15°, (b) 45°, and (c) 60°.

numerical simulation of the transformed medium is suggested using the active EMM in the form of discretization and truncation. The tunable effective mass density is accomplished by applying an adjustable electric field in an ER elastomer under shear mode deformation. Finally, the numerical simulation is conducted to demonstrate tunability and flexibility of the proposed waveguide over a broad frequency range and various steering directions without altering the microstructures. The realization of the flexural waveguide opens new avenues for designing versatile compact acoustic components and have potential applications in a large variety of the fields such as damage detection and structural health monitoring.

Declaration of conflicting interests

The authors declared no potential conflicts of interest with respect to the research, authorship, and/or publication of this article.

Funding

This work was supported by the Air Force Office of Scientific Research under Grant No. AF 9550-15-1-0061 with Program Manager Dr Byung-Lip (Les) Lee.

References

Baz A (2009) The structure of an active acoustic metamaterial with tunable effective density. *New Journal of Physics* 11: 123010.

Chang Z, Hu J, Hu GK, et al. (2011) Controlling elastic waves with isotropic materials. *Applied Physics Letters* 98: 121904.

Chen HY and Chan CT (2007) Acoustic cloaking in three dimensions using acoustic metamaterials. *Applied Physics Letters* 91: 183518.

Chen HY and Chan CT (2010) Acoustic cloaking and transformation acoustics. *Journal of Physics D: Applied Physics* 43: 113001.

Chen YY, Huang GL and Sun CT (2014) Band gap control in an active elastic metamaterial with negative capacitance

Downloaded from jim.sagepub.com by guest on July 28, 2015

piezoelectric shunting. *Journal of Vibration and Acoustics* 136: 061008.

Christensen J and De Abajo F (2012) Anisotropic metamaterials for full control of acoustic waves. *Physical Review Letters* 108: 124301.

Farhat M, Guenneau S and Enoch S (2009) Ultrabroadband elastic cloaking in thin plates. *Physical Review Letters* 103: 024301.

Greenleaf A, Kurylev Y, Lassas M, et al. (2009) Cloaking devices, electromagnetic wormholes, and transformation optics. *SIAM Review* 51: 3–33.

Guo N and Cawley P (1993) The interaction of Lamb waves with delaminations in composite laminates. *Journal of the Acoustical Society of America* 94: 2240–2246.

Hu J, Chang Z and Hu GK (2011) Approximate method for controlling solid elastic waves by transformation media. *Physical Review B: Condensed Matter and Materials Physics* 84: 201101(R).

Huang HH and Sun CT (2009) Wave attenuation mechanism in an acoustic metamaterial with negative effective mass density *New Journal of Physics* 11: 013003.

Huang HH, Sun CT and Huang GL (2009) On the negative effective mass density in acoustic metamaterials. *International Journal of Engineering Science* 47: 610–617.

Leissa AW (1969) *Vibrations of plates report*. NASA SP-160. Available at: http://ntrs.nasa.gov/archive/nasa/casi.ntrs.nasa.gov/19700009156.pdf

Lemistre M and Balageas D (2001) Structural health monitoring system based on diffracted Lamb wave analysis by multiresolution processing. *Smart Materials and Structures* 10: 504–511.

Liu B and Shaw MT (2001) Electrorheology of filled silicone elastomers. *Journal of Rheology* 45: 641–657.

Liu XN, Hu GK, Huang GL, et al. (2011) An elastic metamaterial with simultaneously negative mass density and bulk modulus. *Applied Physics Letters* 98: 251907.

Milton GW, Briane M and Willis JR (2006) On cloaking for elasticity and physical equations with a transformation invariant form. *New Journal of Physics* 8: 248.

Pendry JB, Shurig D and Smith DR (2006) Controlling electromagnetic fields. *Science* 312: 1780–1782.

Schmiele M, Varma VS, Rockstuhl C, et al. (2010) Designing optical elements from isotropic materials by using transformation optics. *Physical Review A: Atomic, Molecular, and Optical Physics* 81: 033837.

Tang H, Luo C and Zhao X (2004) Tunable characteristics of a flexible thin electrorheological layer for low frequency acoustic waves. *Journal of Physics D: Applied Physics* 37: 2331–2336.

Wei KX, Bai Q, Meng G, et al. (2011) Vibration characteristics of electrorheological elastomer sandwich beams. *Smart Materials and Structures* 20: 055012.

Wu TT, Chen YT, Sun JH, et al. (2011) Focusing of the lowest antisymmetric Lamb wave in a gradient-index phononic crystal plate. *Applied Physics Letters* 98: 171911.

Xu Z and Wu F (2014) Elastic band gaps of magnetorheological elastomer vibration isolators. *Journal of Intelligent Material Systems and Structures*. Epub ahead of print 18 May 2014. DOI: 10.1177/1045389X14535014.

Yan X, Zhu R, Huang GL, et al (2013) Focusing guided waves using surface bonded elastic metamaterials. *Applied Physics Letters* 103: 121901.

Yeh JY (2007) Control analysis of the tunable phononic crystal with electrorheological material. *Physica B: Condensed Matter* 400: 137–144.

Zhou XL and Chen CQ (2013) Tuning the locally resonant phononic band structures of two-dimensional periodic electroactive composites. *Physica B: Condensed Matter* 431: 23–31.

Zhu R, Huang GL and Yuan FG (2013) Fast damage imaging using the time-reversal technique in the frequency–wavenumber domain. *Smart Materials and Structures* 22: 075028.

Zhu R, Huang GL, Huang HH, et al. (2011) Experimental and numerical study of guided wave propagation in a thin metamaterial plate. *Physics Letters A* 375: 2863–2867.

Zhu R, Liu XN, Hu GK, et al. (2014) A chiral elastic metamaterial beam for broadband vibration suppression. *Journal of Sound and Vibration* 333: 2759–2773.

Downloaded from jim.sagepub.com by guest on July 28, 2015